

IRSTI 47.17.25

The abundances of heavy elements in BL138 – red giant of local group fornax dwarf spheroidal galaxy

V.F. Gopka¹, A.V. Yushchenko^{2*}, V.A. Yushchenko¹, A.V. Shavrina³, S.M. Andrievsky^{1,4},
Y. Jeong⁵ and E.P. Shereta¹

¹*Department of Astronomy and Astronomical Observatory, Odessa National University,
1, Marazliyvska St., Odessa, UA-65014, Ukraine*

²*Astrocamp Contents Research Institute, Goyang, 10329, Republic of Korea*

³*Main Astronomical Observatory, National Academy of Sciences of Ukraine, Kyiv, 03143 Ukraine*

⁴*GEPI, Observatoire de Paris-Meudon, CNRS, Universite Paris Diderot,
F-92125, Meudon Cedex, France*

⁵*Daeyang College, Sejong University, Seoul 05006, Republic of Korea*

*e-mail address: avyushchenko@gmail.com

Using the spectrum obtained with FLAMES/GIRAFFE multi-object spectrograph installed at ESO Very Large Telescope we investigated the absorption lines of heavy elements in the spectrum of BL138. This red giant star belongs to one of the Local Group members – Fornax dwarf spheroidal galaxy. The abundances of 12 stable chemical elements, namely Y, Zr, Nb, Mo, Ru, La, Ce, Pr, Nd, Eu, Dy, Er, Lu, and Hf. The abundance of radioactive elements Ac and Th are also investigated. The analysis of these abundances and also previously published investigation of BL138 allowed claiming that the distribution of abundances is different from that in the solar photosphere. The signs of r-process in the abundance pattern of BL138 are not important. The production of elements from barium to hafnium can be explained by s-process. The abundances of elements from yttrium to ruthenium are lower than it can be expected in the case of s-process synthesis. That is why it can be expected that several nuclear processes took place in the synthesis of these elements. The possibility of detection the actinium absorption line in the spectrum of BL138 clearly indicate the possibility of physical process which results in continuous production of actinium in the atmosphere of BL138. The actinium abundance can be close to $\log N(\text{Ac})=1.9$. It can be the result of hydrogen accretion from interstellar medium on stellar photosphere. The trends of abundances with second ionization potentials of corresponding chemical elements, and also by the emissions in the profiles of hydrogen H α line confirm this identification.

Key words: fornax dwarf galaxy, late-type stars, BL138, nuclear reactions, nucleosynthesis, abundances of chemical elements, actinium.

PACS numbers: 97.10.Tk, 97.20.Li, 98.56.Wm, 98.80.Ft.

1 Introduction

Our understanding of the structure, evolution and chemical composition of the Universe is based on the stellar abundance patterns as on one of the most important keystones. The modern theory of stellar evolution was created by Burbidge et al. [1, here after B2FH]. Later Fowler [2] doubted the cosmological production of helium. It was found that the energy density of cosmic microwave background radiation, namely $\sim 4.5 \times 10^{-13}$ erg cm⁻³, is equal to the energy output of helium production in stars and the hot phase of the Universe evolution is not necessary. Cosmic microwave background in

this case can be explained as a reemission of stellar radiation by interstellar and intergalactic dust [3]. Burbidge [4] summarized the series of their papers on stellar evolution in the frames of cyclic Universe with typical time scale not less than 10^{11} - 10^{12} years or even longer. The modern epoch is the phase of expansion.

In accordance to B2FH [1] all chemical elements heavier than Cu ($Z=29$) were created mainly in r- and s-processes. s-process takes place mainly in stars, more specifically in red giants; the astrophysical sites of r-process are still under discussion [5]. Many other nuclear processes were proposed also. As an example it is possible to

mention the Thorne-Żytkow objects [6] which are explained as neutron star under intensive accretion from secondary companion, the huge overabundances of elements with atomic numbers in the range from 30 to 50 are expected [7]. The recent observations of gamma ray burst GRB170817A and its afterglow [8] confirms one of the previously proposed r-process scenarios – namely the merging of two neutron stars, with r-process nucleosynthesis going to the third r-process peak (the corresponding atomic masses are close to $A=195$).

It should be mentioned that B2FH theory was based only on the abundances of chemical elements in Solar system and in Milky Way stars. The first investigations of high resolution spectra in other Local Group galaxies started in the 80th of previous century. Fornax dwarf spheroidal galaxy is one of the nearest satellites of our Galaxy, the member of Local Group. Here after we show preliminary results of the investigation of heavy element abundances in the atmosphere of BL138 – red giant of this satellite. In the subsequent sections we describe the observations and the abundance determinations, compare the derived abundances with previous investigations and solar system r- and s-process isotopic composition, and discuss the obtained results.

2 Observations, Data Reduction and Abundance Determination

We used the spectrum of BL138 obtained by Letarte et al. [9] using FLAMES/GIRAFFE multi-object spectrograph with high resolution setup installed at the Very Large Telescope of European Southern Observatory. The observation was made with spectral resolution $R=30,000$ in the wavelength intervals 5339-5608, 6119-6397, and 6308-6689 Å, signal to noise ratio is in the range from 30 to 100 for different wavelengths. Initial reduction of the spectrum was made by the authors of [9] and is described in this paper.

We calculated synthetic spectrum of BL138 for the whole wavelength range and compare it with observed spectrum. For synthetic spectra

calculations we used Kurucz program SYNTHE [10] and atmosphere parameters of BL138 derived by [9]: effective temperature $T_{\text{eff}}=3939$ K, surface gravity $\log g=0.71$, microturbulent velocity $v_{\text{micro}}=2.3$ km s⁻¹, metallicity $[\text{Fe}/\text{H}]=-1.01$. It allowed us to make the identification of absorption lines of heavy elements, namely elements with atomic numbers $Z>30$.

Comparison of observed and synthetic spectra, identification of nonblended spectral lines, and measurements of equivalent widths of these lines were made using URAN software [11]. Abundances of chemical elements were found with Kurucz [10] WIDTH9 program. Synthetic spectra calculations were made with Kurucz [10] SYNTHE program.

Table 1 contains the list of identified lines of heavy elements in the spectrum of BL138. The columns of the table contain the identification of line, the wavelength, the measured equivalent width, the used oscillator strength, the energy of low level, and the calculated abundances in the scale $\log N(\text{H})=12$. The last column contains the equivalent widths of the line, measured by Letarte et al. [9]. The equivalent widths and abundances for actinium and thorium lines are discussed as only the upper limits.

In the next section we will provide the abundance of actinium calculated with spectrum synthesis method, found with using URAN software [11] and Kurucz [10] SYNTHE program in semiautomatic mode. More detailed description of used method can be found in our previous publications.

Table 2 shows the mean abundances of chemical elements in the atmosphere of BL138. This table contains also the results, found by Letarte et al. [9]. The columns of the tables are the identification of chemical element and its ionization stage, the mean abundances with respect to the solar photosphere value taken from [12], the errors, and the number of individual spectral lines, used for this calculation in this study and in Letarte et al. [9].

Figure 1 illustrates the abundance pattern of BL138 derived in our research, and also in Letarte et al. [9].

Table 1 – Lines of heavy elements in the spectrum of BL138

Ident.	Wavelength (Å)	Eq. Width (mÅ)	log gf	E _{low} (eV)	logN	Eq. Width (mÅ) [9]
Y I	6222.578	21.5	-1.70	0.000	1.149	–
Y I	6435.004	58.1	-0.82	0.066	0.905	–
Y II	5402.774	35.5	-0.51	1.839	1.027	32.2
Y II	5509.895	109.0	-1.01	0.992	1.396	–
Y II	5544.611	22.3	-1.09	1.738	1.187	–
Zr I	5385.151	52.2	-0.71	0.519	1.381	–
Zr I	5502.149	22.3	-1.18	0.999	2.106	–
Zr I	6121.922	20.0	-1.16	0.999	1.973	–
Zr I	6127.457	110.0	-1.06	0.154	1.669	–
Zr I	6134.548	87.3	-1.28	0.000	1.403	–
Zr I	6143.203	128.0	-1.10	0.071	1.769	–
Nb I	5350.722	24.4	-0.91	0.267	0.544	–
Mo I	5533.031	72.0	-0.07	1.335	0.892	–
Mo I	5570.444	62.4	-0.34	1.335	1.040	–
Mo I	6619.134	12.9	-1.25	1.335	0.981	–
Ru I	5484.328	13.7	-1.66	1.002	1.285	–
Ru I	5456.126	27.5	-1.62	1.139	1.804	–
La II	6320.376	83.5	-1.61	0.173	0.608	80.4
La II	6390.477	67.0	-1.41	0.321	0.424	65.2
Ce II	5582.556	12.0	-0.57	1.666	1.210	–
Ce II	6570.799	20.3	-2.06	0.529	1.296	–
Pr II	5513.562	14.2	-0.81	0.923	0.393	–
Pr II	6566.762	17.0	-1.72	0.216	0.293	–
Nd II	5442.264	64.0	-0.91	0.680	0.910	–
Nd II	5485.696	41.0	-0.12	1.264	0.626	36.3
Nd II	5508.398	27.3	-1.23	0.859	0.916	–
Nd II	5533.820	23.2	-1.23	0.559	0.396	–
Nd II	5581.591	27.4	-1.19	0.859	0.870	–
Nd II	5595.802	17.5	-1.53	0.859	0.973	–
Nd II	5603.648	37.7	-1.69	0.380	0.861	–
Nd II	6183.897	30.0	-0.92	1.160	1.050	–
Nd II	6248.274	24.4	-1.05	1.225	1.154	–
Nd II	6539.924	19.9	-1.90	0.745	1.192	–
Nd II	6637.187	15.4	-0.84	1.452	1.015	–
Eu II	6645.064	72.0	0.20	1.380	0.201	69.0
Dy II	5368.200	14.0	-2.81	0.103	0.852	–
Dy II	5399.936	12.0	-2.49	0.538	1.080	–
Er II	5414.631	22.7	-2.50	0.000	0.513	–
Lu II	6221.890	43.2	-0.76	1.542	-0.059	–
Hf I	5438.741	17.6	-2.72	0.000	1.095	–
Hf I	6185.125	20.1	-2.48	0.000	0.840	–
Hf I	6386.231	18.0	-2.29	0.292	1.044	–
Hf II	6248.924	12.9	-1.62	1.497	0.954	–
Ac II	6164.750	≤14.3	-0.85	0.588	≤-1.586	–
Th II	6619.944	≤4.0	-1.81	0.514	≤-0.505	–
Th II	5488.629	≤5.2	-2.61	0.000	≤-0.270	–
Th II	6619.944	≤6.0	-1.81	0.514	≤-0.320	–

Table 2 – The mean abundances of heavy elements in the atmosphere of BL138

	This investigation			Letarte et al. [9]		
	$\Delta\log N$	σ	n	$\Delta\log N$	σ	n
Mg I				-1.09	0.10	3
Si I				-0.72	0.17	1
Ca I				-1.19	0.08	9
Ti I				-1.11	0.06	8
Ti II				-0.86	0.12	3
Cr I				-1.28	0.17	1
Fe I				-1.01	0.06	43
Fe II				-0.58	0.13	5
Ni I				-1.11	0.08	14
Y I	-1.14	0.12	2			
Y II	-0.97	0.15	3	-1.16	0.17	1
Zr I	-0.83	0.27	6			
Nb I	-0.89		1			
Mo I	-0.87	0.06	3			
Ru I	-0.17	0.26	2			
Ba II				-0.54	0.14	2
La II	-0.56	0.09	2	-0.59	0.17	1
Ce II	-0.29	0.04	2			
Pr II	-0.34	0.05	2			
Nd II	-0.47	0.22	11	-0.78	0.14	3
Eu II	-0.28		1	-0.28	0.17	1
Dy II	-0.09	0.11	2			
Er II	-0.38		1			
Lu II	-0.12		1			
Hf I	0.18	0.11	3			
Hf II	0.14		1			
Ac II	≤ -1.60		1			
Th II	≤ -0.49		3			

3 Discussion

Tables 1, 2 and Figure 1 show the good coincidence of our results with values obtained by Letarte et al. [9]. The star clearly exhibits the enhancement of heavy elements abundances with respect to α -process elements. The increased number of identified lines of heavy elements allows us to confirm the Letarte et al. [9] conclusion that the nucleosynthesis in AGBs is responsible for 90% of the neutron-capture elements via the s-process and only 10% is contributed by the r-process. Note

that this conclusion is based in the measured abundances of only few heavy elements, namely on the abundances of yttrium, barium, lanthanum, neodymium and europium, but these abundances were found in the atmospheres of 81 stars.

We have the abundances of only 12 stable heavy elements but measured only in one star. We compare our abundances in the photosphere of BL138 and the abundances obtained in [9] with solar system r- and s-process isotopes abundance distribution taken from [13]. The result is shown in Figure 2.

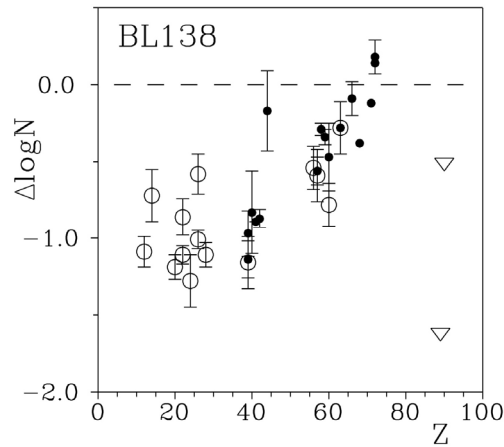


Figure 1 – The abundances of chemical elements in the photosphere of BL138 with respect to solar photosphere values. Filled circles – this investigation, open circles – Letarte et al. [9]. Triangles – upper limits for actinium and thorium abundances. Dashed line marks the solar abundances. Note that the solar system actinium abundance is not known, that is why the actinium point shows the upper limit of actinium abundance in the absolute scale $\log N(\text{Ac}) \leq 1.6$ where $\log N(\text{H}) = 12$

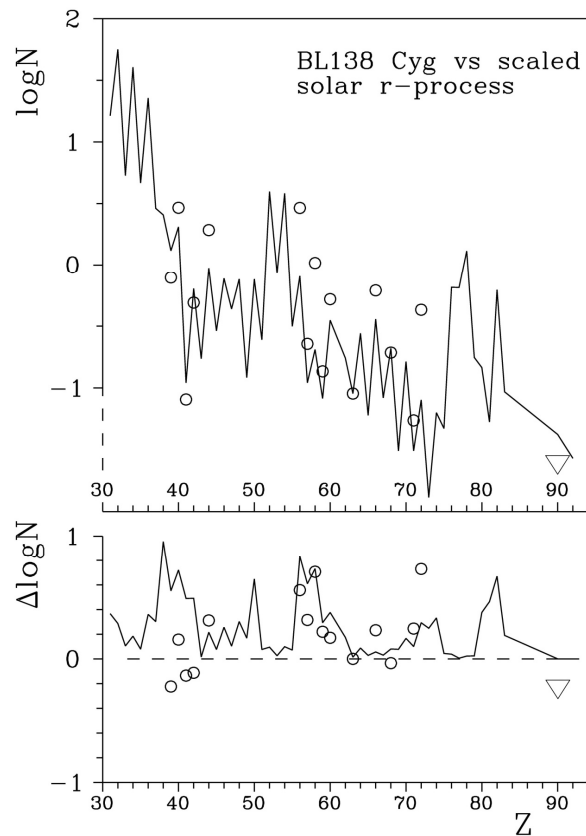


Figure 2 – Upper panel: the comparison of the surface abundances in BL138 (circles) with the solar system r-process abundance distribution [13] scaled at the observed Eu abundance (line). Triangle is the upper limit of thorium abundance. Bottom panel: the differences of observed abundances in BL138 and scaled solar system r-process abundances (circles). The line is the deviations of solar photosphere abundances from the solar r-process abundance distribution. The maximums of this curve are expected for the elements with the highest relative s-process contributions. The actinium abundance is not shown

The upper panel of this figure confirms that r-process is not important in the abundance pattern of BL138. The bottom panel indicates the increased abundances of part of s-process elements, namely, barium, lanthanides and hafnium. But the light s-process elements (yttrium to ruthenium) are relatively less abundant. s-process cannot start from barium. The abundances of elements with atomic numbers less than 56 should confirm the s-process abundance distribution, but we found the relative underabundances of these elements. It can be the result of different scenario of chemical elements synthesis in the atmosphere of BL138, and, maybe, in the Fornax dwarf galaxy.

Note that two groups of chemical elements namely the elements from yttrium to ruthenium and from barium to hafnium were clearly synthesized in different nuclear processes or under the different combinations of already known processes.

Gopka et al. [14] identified two lines of actinium in the spectrum of red supergiant RM_1-667 which belongs to other Galaxy satellite – Large Magellanic Cloud. As the longest-live actinium isotope has a half-life near 20 years it is necessary to suppose the existence of unknown physical process to generate the atoms of this unstable chemical element in the stellar atmosphere continuously. In [14] it was also pointed that one of the actinium lines can be identified in the spectrum of BL138, and that the profile of hydrogen H α line is strongly disturbed in the spectra of both stars: RM_1-667 and BL138. It was supposed that this anomaly can be the result of accretion of hydrogen atoms from interstellar medium on the surface of both RM_1-667 and BL138.

Figure 3 shows the spectrum of BL138 in the vicinity of actinium line. Synthetic spectrum method allows the stronger limitation on the abundance of this element. The actinium abundance can be close to $\log N(\text{Ac}) = -1.9$ in the scale $\log N(\text{H}) = 12$. We used the recent investigation of oscillator strengths and partition functions for actinium [15, 16] and the new value of ionization potential of neutral actinium (5.38 eV) determined in 2012 [17]. Note that the actinium abundance in the atmosphere of RM_1-667 is $\log N(\text{Ac}) = -1.3 \pm 0.1$ [14]. It means that the actinium abundance in the atmosphere of BL138 is at least 0.6 dex lower than the abundance of this element in RM_1-667.

Hydrogen line H α and other regions of BL138 spectrum exhibit the signs of possible emissions, more detailed inspection of all Fornax red giant stars is necessary to confirm or to reject the existence of

unknown process which can continuously generate actinium in stellar atmosphere.

Figure 4 shows the relative abundances of chemical elements in the atmosphere of BL138 as a function of second ionization potentials of these elements. Greenstein [18] was the first who found these dependence and explain it as a result of charge-exchange reactions between hydrogen atoms and the atoms of other chemical elements with second ionization potentials close to the ionization potential of hydrogen atom, namely to 13.6 eV.

As a result the atoms can leave the star, produce the underabundance of certain chemical element and also brake the stellar rotational velocity. More detailed theory of this process was proposed in early 70th of the former century [19, 20] but not developed in later investigations. One of the possible results of this scenario was found to be the decreasing of rotational velocities of magnetic chemically peculiar stars of the upper main sequence.

The energy released as a result of braking the rotational velocities from several hundred kilometres per second to the observed close to zero velocity values is similar to the total energy of Galactic cosmic rays with energies less than 200 MeV/nucleon. Böhm-Vitense [21] and Yushchenko et al. [22] showed the recent observational results which can be explained by this effect. In few words the signs of this scenario were found in several hundreds usual main sequence stars, including the stars without strong magnetic fields. The detailed physical picture of this mechanism needs improvement, first of all it is necessary to investigate its observational signs in different type stars.

Figure 4 confirms the relative deficiency of chemical elements with second ionization potentials close to 13.6 eV in the atmosphere of BL138. It also confirms the trends of abundances with second ionization potentials similar to those published by Yushchenko et al. [22]. Note that Yushchenko et al. [22], as well as Bohm-Vitence [21] found these dependencies for stars with radiative photospheres, but Kang et al. [23] showed that similar dependencies can exist in convective photospheres under the condition of strong accretion of interstellar or circumstellar matter. It should be mentioned, that the energy transport in the photospheres of red giant stars are mainly radiative, that is why even small peculiarities of chemical composition created by any physical scenario can be conserved for long time.

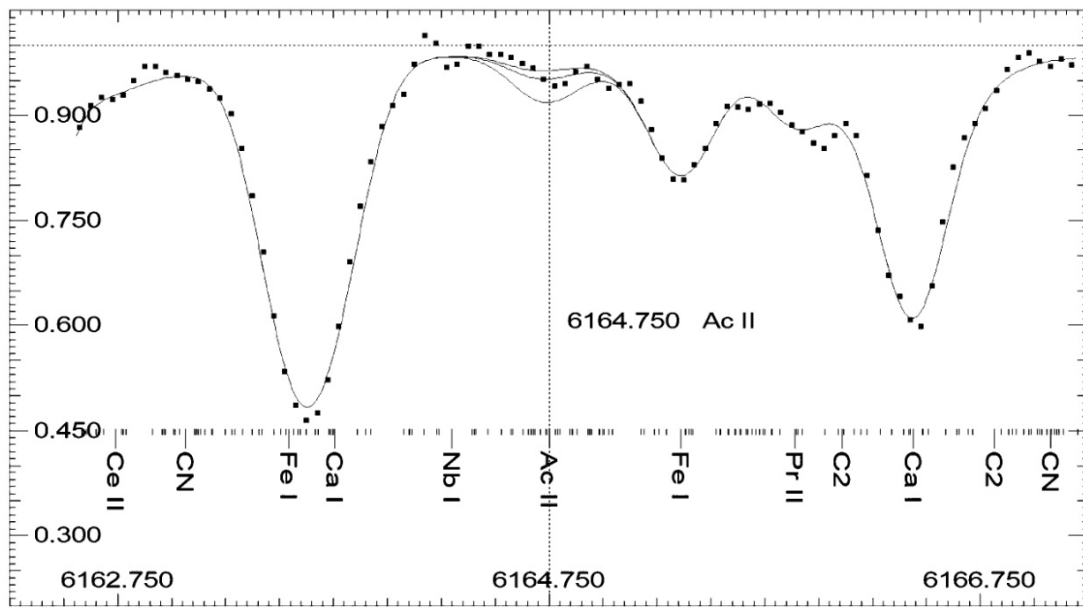


Figure 3 – The plot of BL138 spectrum in the vicinity of actinium line 6164.75 Å. The axes are wavelength and relative flux. The points denote the observed spectrum, the lines – synthetic spectra. The positions of the spectral lines, which were taken into account in the calculations, are marked in the bottom part of the figure by short and long dashes (faint and strong lines, respectively). The identifications are shown for the strongest lines. Three synthetic spectra in the vicinity of actinium line were calculated with the best abundance of this element, and the abundances increased and decreased by 0.5 dex. The best actinium abundances is $\log N(\text{Ac}) = -1.9$ in the scale $\log N(\text{H}) = 12$,

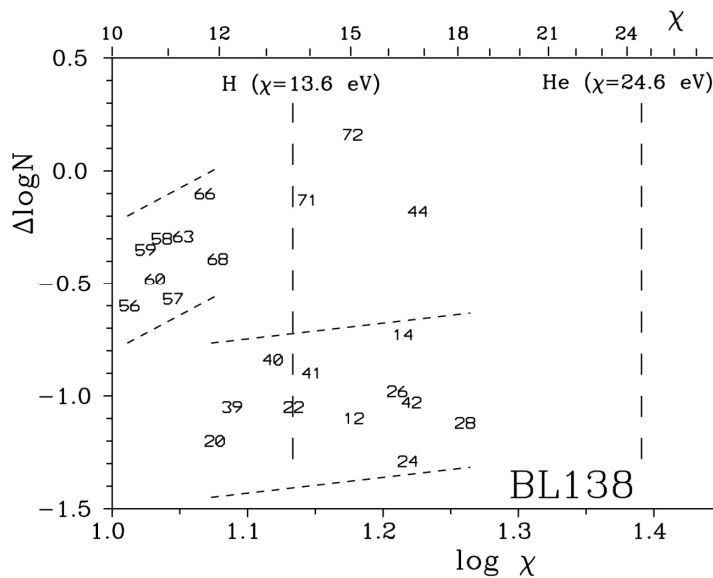


Figure 4 – Plot of relative surface abundances of chemical elements in BL138 (with respect to the solar photosphere abundances) as a function of the second ionization potentials (χ) of these elements. The positions of elements are marked by atomic numbers. The positions of the ionization energies of hydrogen and helium are marked by vertical dashed lines. The logarithms of ionization potentials are shown on the bottom parts of the panels and the potentials themselves on the upper parts. The inclined dashed lines define the possible trends.

The relatively high abundances of several chemical elements, namely lutetium, hafnium and ruthenium can not be explained by this hypothesis. As it is shown in Figure 2 hafnium is located at one of the peaks of s-process abundance distribution. The overabundance of ruthenium as well as the relatively low abundances of yttrium to molybdenum elements can not be easily explained by any known nuclear process.

Of course, different physical scenarios should take place in the atmosphere of any star. Maybe the chemical composition of BL138, as well as of other Fornax dwarf spheroidal galaxy stars can be the result of unusual combination of well known physical processes, but the relative parts of these processes are different in giant spiral galaxy – in our Milky Way and in Fornax dwarf spheroidal galaxy.

5 Conclusions

In present paper we derived the abundances of 12 stable heavy elements in the atmosphere of BL138, and also discuss the radioactive elements, namely we found the actinium abundance and limit the abundance of thorium. Comparison of our results with earlier investigation of this star showed a good coincidence. The analysis of abundance

pattern allowed the conclusion that r- and s-processes of nuclear synthesis can not fully describe the chemical composition of BL138. The most important differences are found for chemical elements from yttrium to ruthenium. It can be the result of unknown nuclear processes which took place in the evolutionary history of Fornax dwarf spheroidal galaxy.

The possible detection of actinium in the atmosphere of BL138 also confirms the necessity of new scenarios for explanation of observed abundances. One of these scenarios can be the accretion of hydrogen from interstellar medium. The signs of this accretion are observed in the distribution of elemental abundances with respect to second ionization potentials of these elements and in the profiles of strong lines.

The careful investigation of BL138 and other Fornax galaxy stars with spectrum synthesis method can confirm or reject the possible differences in evolutionary history of Milky Way and its satellites.

Acknowledgments

The authors express their gratitude to Vanessa Hill for providing us the observed spectrum of BL138.

References

1. E.M. Burbidge, G.R. Burbidge, W.A. Fowler, F. Synthesis of the elements in stars // *Reviews of Modern Physics* -1957. – Vol. 29. – P. 547-650.
2. W.A. Fowler. How now, no cosmological helium? // *Comments on Astrophysics and Space Physics*. – 1970. – Vol. 2. – P. 134-137.
3. J.V. Narlikar, R.G. Vishwakarma, A. Hajian, T. Souradeep, G. Burbidge, F. Hoyle. Inhomogeneities in the microwave background radiation interpreted within the framework of the quasi-steady state cosmology // *The Astrophysical Journal*. – 2003. – Vol. 585. – P. 1-11.
4. G. Burbidge. B2FH, the cosmic microwave background and cosmology // *Publications of the Astronomical Society of Australia*. – 2008. – Vol. 25. – P. 30-35.
5. G. Wallerstein et al. Synthesis of the elements in stars: forty years of progress // *Reviews of Modern Physics*. – 1997. – Vol. 69. – P. 995-1084.
6. K.S. Thorne, A.N. Żytkow. Red giants and supergiants with degenerate neutron cores // *The Astrophysical Journal*. – 1975. – Vol. 199. – P. L19-L24.
7. G.T. Biehle. Observational prospects for massive stars with degenerate neutron cores // *The Astrophysical Journal*. – 1994. – Vol. 420. – P. 364-373.
8. N.R. Tanvir et al. The emergence of a lanthanide-rich kilonova following the merger of two neutron stars // *The Astrophysical Journal* – 2017. – Vol. 848. – P. L27-L35.
9. B. Letarte et al. A high-resolution VLT/FLAMES study of individual stars in the centre of the Fornax dwarf spheroidal galaxy // *Astronomy and Astrophysics*. – 2010. – Vol. 523. – A17-A56.
10. R.L. Kurucz. Atomic data for opacity calculations // Kurucz CD-ROM – 1993. – No. 1–2. (Smithsonian Astrophys. Obs., Cambridge, MA, 1993).
11. A.V. Yushchenko. URAN: A software system for the analysis of stellar spectra // *Proc. 20th Stellar Conf. of the Czech and Slovak Astronomical Inst., Brno, Czech Republic, Nov. 5–7, 1997, Ed. by J. Dušek (Nicolaus Copernicus Obs. and Planetarium Brno, 1998).* -P. 201–204.

12. N. Grevesse, P. Scott, M. Asplund, A.J. Sauval. The elemental composition of the Sun. III. The heavy elements Cu to Th // *Astronomy and Astrophysics*. – 2015. – Vol. 573. – A27.
13. J. Simmerer, C. Sneden, J.J. Cowan, J. Collier, V.M. Woolf, J.E. Lawler. The rise of the s-process in the galaxy // *The Astrophysical Journal*. – 2004. – Vol. 617. – P. 1091–1114.
14. V.F. Gopka et al. Actinium abundance in the atmospheres of three red supergiants in the Magellanic Clouds // *Kinematics and Physics of Celestial Bodies*. – 2018. – Vol. 34. – P. 123–133.
15. P. Quinet, C. Argante, V. Fivet, C. Terranova, A.V. Yushchenko, É. Biémont. Atomic data for radioactive elements Ra I, Ra II, Ac I and Ac II and application to their detection in HD 101065 and HR 465 // *Astronomy and Astrophysics*. – 2007. – Vol. 474. – P. 307–314.
16. G. Urer, L. Ozdemir. The level structure of singly-ionized actinium // *J. Korean Phys. Soc.* – 2012. – Vol. 61. – P. 353–358.
17. J. Roßnagel, S. Raeder, A. Hakimi, R. Ferrer, N. Trautmann, K. Wendt. Determination of the first ionization potential of actinium // *Physical Review A*. – 2012. – Vol. 85. – P. 012525.
18. J.L. Greenstein. Analysis of the metallic-line stars. II. // *The Astrophysical Journal*. – 1949. – Vol. 109. – P. 121–138.
19. O. Havnes. Abundances and acceleration mechanisms of cosmic rays // *Nature* – 1971. – Vol. 229. P. 548–549.
20. O. Havnes, P.S. Conti. Magnetic accretion processes in peculiar A stars // *Astronomy and Astrophysics*. – 1971. Vol. – 14. -P. 1–11.
21. E. Böhm-Vitense. The puzzle of the metallic line stars // *The Publications of the Astronomical Society of the Pacific*. – 2006. – Vol. 118. – P. 419-435.
22. A.V. Yushchenko, V.F. Gopka, Y.-W. Kang et al. The chemical composition of ρ Puppis and the signs of accretion in the atmospheres of B–F-type stars // *The Astronomical Journal*. – 2015. – Vol. 149. – A.59 (22 p.).
23. Y.-W. Kang, A.V. Yushchenko, K. Hong, E.F. Guinan, V.F. Gopka. Signs of accretion in the abundance patterns of the components of the RS CVn-type eclipsing binary star LX Persei // *The Astronomical Journal*. – 2013. – Vol. 145. – A167 (15 pp.).